Carbohydrate Polymers 204 (2019) 232–237

Contents lists available at ScienceDirect

Carbohydrate Polymers

journal homepage: www.elsevier.com/locate/carbpol

The fibrils untwisting limits the rate of cellulose nitration process☆

Sergey N. Nikolsky[a], Dmitry V. Zlenko[a,b,*], Valery P. Melnikov[a], Sergey V. Stovbun[a]

[a] N.N. Semenov Institute of Chemical Physics RAS, Moscow, Russia
[b] Biological Faculty of M.V. Lomonosov Moscow State University, Moscow, Russia

ARTICLE INFO

Keywords:
Cellulose
Nitration
Kinetics
Untwisting

ABSTRACT

The rate of cellulose nitration is lower compared to the low molecular weight substances. Theoretical estimates assess that the rate of the nitrating agents' diffusion cannot provide for the characteristic time of cellulose nitration, as the densely packed regions are too small. However, the electrostatic barrier between the nitrating mixture and the microcrystallites makes the latter inaccessible for the nitronium ion. The cellulose nitration rate decreases and the transformation of elementary fibril structure occurs at the same degree of substitution corresponding to a complete nitration of the fibrils' surface. The supercoiled macromolecules in the elementary fibrils cannot dissociate without untwisting. The fibrils' untwisting as well as their swelling are very slow. Thus, we propose that the nanofibrils' untwisting limits the rate of the nitronium ion transport into the cellulose nanofibrils and, thus, the rate of the nitration reaction as a whole.

1. Introduction

Nitrocellulose is the most important industrial polymer used as a raw material for producing a number of decorative and protective coatings (varnishes) and smokeless propellants. The quality as well as ballistic characteristics of a propellant depend strongly on the homogeneity of nitrocellulose and the nitrogen content in it (Balser et al., 2012) making the process of nitration crucial.

The process of cellulose nitration can not be considered neglecting the cellulose supramolecular structure, as the kinetic of any process in the heterogeneous conditions differs from that in a homogeneous one (Rafeev, Rubtsov, Sorokina, & Chukanov, 1999). The cellulose is structured across four hierarchical levels. The first is the level of macromolecules with the chain length reaching 15 000 monomers in cotton fiber (O'Sullivan, 1997; Somerville, 2006). In the native state, cellulose chains are arranged in the form of 2_1-helices, where each successive residue is turned upside down relative to the previous one (Meader, Atkins, & Happey, 1978). During the nitration, the chains change their packing and untwist to the 5_2-helices (Meader et al., 1978).

The second level embraces the elementary fibrils (nanofibrils), which have a very dense, crystalline structure and do not contain water, lignin, or hemicellulose (O'Sullivan, 1997). The thickness of nanofibrils depends on the origin of cellulose, ranging from 3.5 nm in softwood cellulose (Fernandes et al., 2011; Muhlethaler, 1967) to 5–6 nm in flax cellulose and to 7–9 nm in cotton cellulose (Newman, 1999). The structure of nanofibrils extracted from various plants was resolved by X-ray diffraction (Fernandes et al., 2011; Thomas et al., 2013). Each nanofibril of softwood cellulose, i.e. has a rectangular cross-section and consists of 24 closely packed cellulose chains (Fernandes et al., 2011). The structure of nanofibrils forming directly in the course of cellulose biosynthesis and is determined by the co-arrangement of the cellulose synthase subunits (Saunders & Taylor, 1990; Somerville, 2006). Nanofibrils have a helical structure, but the helix pitch was not determined (Fernandes et al., 2011). Molecular modeling revealed that the twist angle of the thick fibrils is smaller than that of the thin ones, and the helix pitch is about 100 and 250 nm for the softwood and cotton fibrils, respectively (Zhao et al., 2013). It was also reported that the tobacco nanofibrils consist of nine cellulose chains assembled into a three-membered left-handed helix (Ruben & Bokelman, 1987).

The third level comprises microfibrils (O'Sullivan, 1997), where each microfibril is a bundle of nanofibrils glued together via low molecular weight hemicelluloses and lignin (O'Sullivan, 1997). The thickness of microfibrils is about 30–40 nm, and they are often assembled into bundles (Hanley, Giasson, Revol, & Gray, 1992). Microfibrils also have a helical structure, that was directly shown by electron and atomic-force microscopy (Hanley, Revol, Godbout, & Gray, 1997).

The fourth structural level is the cellulose fiber itself or the cell wall made up of several layers of microfibrils. They are not parallel to the long axis of the cell (Preston, 1934) as clearly seen in electron microscopy images (Fig. 1). This provides for the helical structure of the cell

☆ The work was supported by FASO Russia, theme number 45.9, 0082-2014-0011, AAAA-A17-117111600093-8.
* Corresponding author at: Biological Faculty of M.V. Lomonosov Moscow State University, Moscow, Russia.
E-mail address: dvzlenko@gmail.com (D.V. Zlenko).

https://doi.org/10.1016/j.carbpol.2018.10.019
Received 21 June 2018; Received in revised form 6 October 2018; Accepted 6 October 2018
Available online 10 October 2018
0144-8617/

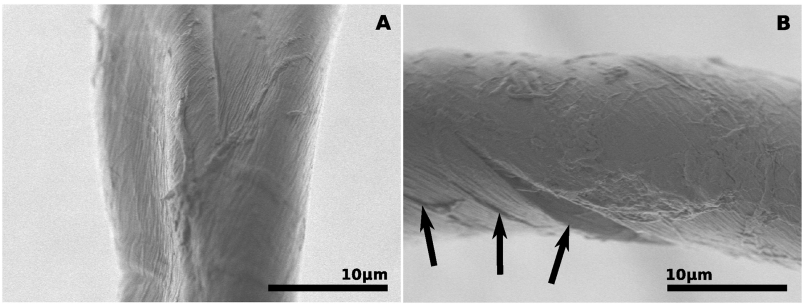

Fig. 1. Electron microscopy images (×3500) of the cotton fibers before nitration (A) and after 60 min treatment with the nitrating mixture at 25 °C. The arrows mark the cracks on the nitrocellulose fiber.

envelope as a whole (O'Sullivan, 1997). Thus, cellulose has a complex supramolecular structure with four helical hierarchical levels.

The cellulose nitration proceeds through substituting the hydrogen of hydroxyl groups by the NO_2-group. In case of all alcohols and amines the nitration reaction proceeds due to the electrophilic attack of the nitronium ion (NO_2^+) on the hydroxyl- or amino-group (Ingold, 1953). The same mechanism was established for cellulose (Short & Munrot, 1993). The active agent (NO_2^+) arises in different reaction mixtures, typically in a concentrated nitric acid:

$$3HNO_3 \leftrightarrow 2NO_3^- + NO_2^+ + H_3O^+$$

In the presence of water, the equilibrium of this reaction is dramatically shifted to the left (Edwards & Fawcett, 1994). The concentration of the nitronium ion can be increased by adding the dehydrating agents, such as sulfuric acid or pentavalent nitrogen oxide. In a 70:20:10 sulfuric acid: nitric acid: water triple mixture, the nitronium ion is formed in the reaction:

$$HNO_3 + 2H_2SO_4 \leftrightarrow NO_2^+ + 2HSO_4^- + H_3O^+$$

These mixtures are widely used in the industry for nitrating various substrates, including glycerol and cellulose. For the homogeneous nitration reactions, the formation of the nitronium ion is a limiting stage (Hughes, Ingold, & Pearson, 1958; Ingold, 1953). The concentration of the nitronium ion in standard nitrating mixtures can be rather high. At low concentrations of water and nitric acid, the latter can be completely dissociated, so the concentration of the nitronium ion can reach several moles per liter (Edwards & Fawcett, 1994). Given that the formation of the nitronium ion is a limiting step, the reaction completes within a few seconds upon its high concentrations (Hughes et al., 1958; Ingold, 1953). This effect was observed for the cellulose fibers surface nitration in mixtures with high NO_2^+ content: the degree of substitution reached 2.3 after one second of nitration and does not grow in further (Short & Munrot, 1993). In this case the nitration affects only the surface of the fibrils that usually leads to the inhomogeneity of the final product (Kovalenko, 1995). Full nitration of cellulose (up to 13.5% of nitrogen or more) takes at least half an hour (Belova et al., 1989; Short & Munro, 1990). The nitration of the wood cellulose disintegrated into individual fibers demonstrated qualitatively higher rates of nitration and the nitrogen content of 12% was achieved within one minute (Sullivan et al., 2018). Nevertheless, the final concentrations of nitrogen exceeding 13% were achieved after 30min of nitration.

The origin of cellulose plays a key role in the effectiveness of the nitration process, the portion of α-cellulose and mechanical properties of the raw, as well as the temperature are also important (Sullivan et al., 2018; Urbansky, 1965). The Alfa grass cellulose nitration demonstrated increase of the nitrogen content in more crystalline samples that was explained by the difference in diffusion of nitrating agents (Trache, Khimeche, Mezroua, & Benziane, 2016). This effect could also be explained by the greater portion of α-cellulose that is known to have crystalline structure and its content strongly affects the yield of nitration (Urbansky, 1965). The latter assumption is confirmed by the results of wood cellulose nitration that demonstrated the inverse relation between nitrating ability and the crystallinity of the initial raw and the direct correlation between the nitrocellulose yield and α-cellulose content (Sullivan et al., 2018).

There are two stages in the kinetics of cellulose nitration reaction. The first stage is the fast one defined by the characteristic time of about a minute or less, while the second stage is slow lasting for half an hour (Belova et al., 1989). For a HNO_3/CH_2Cl_2 nitrating mixture, the rate constant of the fast stage ($6.2 \times 10^{-2}\,s^{-1}$) turned out to be ten times higher than that for the slow one ($5.0 \times 10^{-3}\,s^{-1}$) (Belova et al., 1989). Similar results were reported for the H_2SO_4/HNO_3 classical mixture (Short & Munro, 1990). These two stages can be associated with the nitration of hydroxyl groups located in different spatial domains with various diffusional accessibility (Barbosa, Merquior, & Peixoto, 2005; Belova et al., 1989), and this point of view is generally accepted. The modeling of the cellulose nitration process in the homogeneous approximation suggests that some factors, possibly diffusion, play a key role in this process (Barbosa et al., 2005). The decrease of the reactivity of the cellulose hydroxyl groups in course of nitration was directly introduced into the model describing the wood cellulose nitration, but the nature of this effect was not explained (Sullivan et al., 2018). Yet, the cellulose is a heterogeneous disordered system, so treating it as a homogeneous system is ambiguous. Moreover, it is reasonable to propose that the physicochemical processes in the individual fibers play a key role in controlling the cellulose nitration rate.

According to the X-ray photoelectron spectroscopy, the surface cellulose nitration appears to be very fast process, while the nitration of the bulk of the fiber requires much more time (Short & Munrot, 1993). Moreover, complete nitration of the surface seems to prevent further nitration of the bulk (Short & Munrot, 1993). This observation correlates well with the direct correlation between the heterogeneity of the final nitrocellulose and NO_2^+ concentration (Kovalenko, 1995). This effect was explained by the intense nitration of the fibers surface that hinders further nitration of the fibers interior (Kovalenko, 1995).

In summary, the cellulose nitration rate and effectiveness depend on the nature of the raw and its preliminary treatment, the nitrating mixture content, and temperature. The appropriate combination of the raw treatment and nitrating mixture composition allows to increase the rate of cellulose nitration and obtain rather high nitrogen content (~12%) after several minutes of reaction. Nevertheless, to reach the nitrogen content of about 13.5% or more the reaction takes at leas a half hour. This phenomenon was described qualitatively, while in the models the cellulose pulp was considered as a homogeneous media.

In this work we provide theoretical arguments for the insufficiency of the diffusional restriction to provide for the observed cellulose nitration slowdown at high degrees of substitution. We attempted to embrace the peculiarities of the cellulose supramolecular structure, first and foremost, – its helical nature, to explain the observed rate decrease. As the cellulose chains length does not decrease drastically in course of nitration, the only way for NO_2^+ to reach the elementary fibrils interior

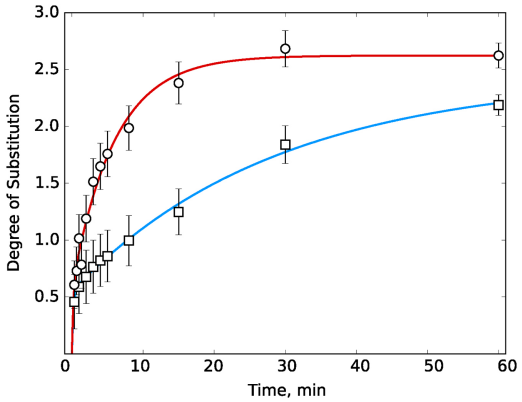

Fig. 2. Kinetics of cotton lint nitration at 295 K (circles) and 278 K (squares), approximated by the sum of two exponentials (red and blue curves). The nitrogen content was measured by elemental analysis.

is the loosening of their structure. Due to the helical structure of the fibrils the loosening can occur only through their untwisting that is rather slow process due to significant length and mass of the cellulose chains. This hypothesis explains the low rate of chemical reaction through its tight relation to the rather slow mechanical process of the polymer matrix reassembling.

2. Materials and methods

Samples of cotton lint containing 95–97% of alpha-cellulose were supplied by OOO Fargona Kimyo Zavodi (Uzbekistan). The raw lint was not additionally treated or modified before experiments. The fraction of alpha-cellulose was determined as the proportion of cellulose insoluble in 17.5% NaOH (Richter, 1929). The molecular weight and the degree of polymerization of the original cellulose were determined by the viscosity of copper-ammonium solution of cellulose (Whorlow, 1980). The molecular weight of nitrocellulose was determined by gel permeation chromatography (GPCV 2000 Waters Alliance chromatograph) (Gert, Matyulko, Shishonok, Zubets, & Kaputskii, 2003), with tetrahydrofuran as an eluent.

A standard nitrating mixture, $HNO_3 : H_2SO_4 : H_2O = 25.4 : 67.4 : 7.2\%$, was used for nitration. Cotton lint samples (0.5 g) were immersed in a 40-fold excess of nitrating mixture at 278 and 295 K. After nitration, the samples were dried under vacuum on a glass filter and immediately washed with a large amount of cool (4 °C) 60% sulfuric acid. The procedure was repeated three times, and then sulfuric acid was neutralized with a 5% bicarbonate solution for 30 min. After neutralization, the samples were washed with distilled water until the neutral pH was achieved. Elemental analysis was performed on a Carlo-Ebra 1106 CHN spectrometer equipped with a gas chromatograph. The nitrogen content in the initial unnitrated cotton lint was negligible.

The structure of the cellulose samples was examined on a JSM-7500F, scanning electron microscope (Jeol, Japan), with the acceleration potential in the range between 0.5 and 1.5 kV. The samples were not covered by a metal film. The cotton fiber diameter was measured using a Leica DMI 6000 optical microscope for fibers immersed in water. 100–150 fibers were measured in each sample, 20–50 measurements per each fiber with a step of ~10 μm along the fiber.

3. Results and discussion

The previous works did not consider the peculiarities of the cellulose supramolecular structure thus failing to describe the details of physical and chemical processes in the cellulose pulp. The kinetics of the diffusion-controlled reactions in wood can be interpreted using the concept of isokinetic zones (Mikhailov, Bel'kova, & Gromov, 1980a,1980). These zones differ by the characteristic times of nitration, ranging over several orders of magnitude, and, therefore, the resulting kinetic has a logarithmic form (polychronous kinetics). However, in view of the above-described peculiarities of the cellulose supramolecular structure, there are only two structural levels in it: the elementary fibrils (nanofibrils) and the microfibrils (O'Sullivan, 1997). The diffusion coefficient of the nitrating agents can be significantly (100 or 1000 times) smaller than in the liquid only the former one, as the nanofibrils have the crystalline structure. This point of view seems to explain, at least qualitatively, the nature of the observed two-exponential kinetics. The regions inside the elementary fibrils and outside them have different NO_2^+ diffusion rates and, thus, different rates of nitration.

Since nitrocellulose retains crystallinity (Meader et al., 1978), the characteristic diffusion coefficient inside the microcrystalline regions can be estimated as $D \sim 10^{-11}$ cm^2/s that is common for solids and crystalline polymers (Murch, 1984). This assumption allows to assess the characteristic time of nitronium ions diffusion into nano- and microfibrils. Using the diameters (R) of the nano- and microfibrils of ~3–9 and ~30–40 nm, respectively (Newman, 1999; O'Sullivan, 1997) we obtain the characteristic times of the diffusion:

$$\tau = \frac{R^2}{6D} = 10^{-2} - 10^{-1}\,\mathrm{s}$$

This value is several orders of magnitude lower than the real observed characteristic time of nitration (tens of minutes (Belova et al., 1989; Short & Munro, 1990)). The diffusion can provide such reaction times if the compacted regions with a solid-like diffusion coefficient would have dimensions of ~2.5 μm. This, however, is not the case for the cellulose pulp, since the micron-size scale corresponds to the thickness of the cell wall (Saren, Serimaa, Andersson, Paakkari, & Pesonen, 2001), that does not have crystalline packing (O'Sullivan, 1997). Otherwise the diffusion coefficient should be about 10^{-16}–10^{-17} cm^2/s to provide the characteristic time of nitration about tens of minutes in case of the observed nanometer-sized microcrystallites. Yet, this value is too small for real solids (Murch, 1984). Thus, the diffusional restrictions can not explain why the slow stage of the cellulose nitration reaction takes place (Fig. 2). If there are no other rate-limiting mechanisms, then the reaction would be completed within a few seconds, as it happens in case of the nitration of low-molecular weight substrates (Hughes et al., 1958; Ingold, 1953).

At the same time, the main nitrating agent is the charged nitronium cation. Its transfer from the reaction mixture with a relatively high dielectric constant into a nanofibril with a lower one involves the overcoming of the electrostatic barrier specified by the Born energy for a point charge. The Born energy (ΔE) of a single charged ion transfer from a nitrating mixture with a dielectric constant of $\varepsilon_1 \sim 100$ (Gillespie & Cole, 1956) into a nanofibril with a dielectric constant of $\varepsilon_2 \sim 3$ (Ishida, Yoshino, Takayanagi, & Irie, 1959) can be estimated as:

$$\Delta E = -\frac{q^2}{8\pi\varepsilon_0 r}\left(\frac{1}{\varepsilon_1} - \frac{1}{\varepsilon_2}\right) \sim 1\,\mathrm{eV}$$

The resulting excessively high value (~40 kT) is comparable to the energy of the covalent bond dissociation, and can be considered as a potential barrier, not just limiting but actually prohibiting the NO_2^+ transfer into the interior of the nanofibril. Indeed, according to the Arrhenius equation describing the dependence of any process rate in general, the rate constant k exponentially depends on the activation energy E_A: $k = A * exp(-\Delta E_A/kT)$, where A – some constant. In case of $E_A \sim 40$ kT, the exponential would be $\sim 10^{-18}$ that would strongly decrease the reaction rate. This means the process of cellulose nitration is bound to stop at the stage, when all the hydroxyl groups located on the surface of the nanofibrils became completely nitrated.

The structure of a nanofibril obtained by the X-ray (Fernandes et al., 2011) allows to estimate roughly the fraction of hydroxyl groups on its surface. There is approximately one half of the cellulose chains inside the fibril of spruce (Fernandes et al., 2011). This allows to estimate the

Table 1
Characteristic times (τ, min) and amplitudes (degree of substitution, A) of the components for cellulose nitration kinetics.

	First stage		Second stage	
	278 K	295 K	278 K	295 K
A	0.56 ± 0.11	0.59 ± 0.09	1.89 ± 0.07	2.04 ± 0.04
τ	0.21 ± 0.09	0.19 ± 0.11	28.8 ± 1.2	5.9 ± 1.1

fraction of the surface hydroxyl groups as one half, that leads to the degree of substitution being 1.5 (Belova et al., 1989) that corresponds to the full nitration of the nanaofibrils' surface. According to the results of Fernandes et al. the spruce nanofibril comprises 24 chains and have the thickness of 3–4 nm, that corresponds well to the earlier X-ray and NMR estimates (Meader et al., 1978; Muhlethaler, 1967). The cotton nanofibrils seem to be thicker (Meader et al., 1978). According to the structure of cellulose synthase complex (Somerville, 2006), the nanofibril can be made up of not more than 36 cellulose chains. Proposing for the 36 chain fibril the same structure as for 24 chain one, the amount of the surface chains would be about one quarter. Therefore, in case of the full nitration of the cotton nanofibrils surface the degree of substitution should be about 0.75. According to the above estimates of the diffusion rate, this part of the hydroxyl groups is accessible for nitrating agents. This suggests the first stage of nitration to be finished at the same nitration rate (0.75), that clearly corresponds to the obtained breakdown of the nitration kinetics into two components (Fig. 2, Table 1). For the cotton cellulose we have obtained the degree of substitution being 0.6 at the end of the first stage (Table 1). This result agrees with the results of the surface nitration observed at high NO_2^+ concentrations (Kovalenko, 1995; Sullivan et al., 2018). The *V. Ventricosa* cell wall fibrils acetylation proceeds in the same way: acetylation occur exclusively on the surface, while the core of the fibril remains unreacted (Sasi & Chanzy, 1995).

Using the kinetics measured at different temperatures allowed to assess the thermodynamical parameters of the nitration process at different stages. The activation energy at the first stage was very small. We can only specify that it did not exceed several kJ per mole. This result corresponds well with the reported small activation energy of the reaction between the nitronium ion and the hydroxyl-group (Hughes et al., 1958; Ingold, 1953). On the contrary, the activation energy of the second stage is significant and equals ~60 kJ/mole. This value can be easily related to the energy necessary for the cellulose chains dissociation during the swelling and untwisting processes.

The signs of the crystalline cellulose trinitrate in the form of the peak at 12° (Meader et al., 1978) appear in the X-ray diffractograms already after 1 min of nitration (Fig. 3) at the degree of substitution ranging between 0.5 and 1.0 (Fig. 2), while this peak is absent at the lower degrees of substitution. As far as the additional peak appears at smaller scattering angles, it corresponds to the appearance of some new Bragg scattering planes located at larger distances from each other, than it was in the raw cotton. Thus, the appearance of the 12° peak can be interpreted as cellulose swelling, related to the volume increase induced by the three-fold larger volume of the nitro-group as compared to the hydroxy-group. We propose that this swelling, in turn, is associated with nitrating the interior of the cellulose elementary fibrils.

Since the nitration reaction proceeds beyond the first stage, there must be a mechanism allowing NO_2^+ to penetrate into the bulk of the fibril. Given that the cellulose nanofibrils have a supercoiled structure, the process of dissociating the cellulose chains is prohibited due to their multiple twists and overlaps. Thus, to move the cellulose chains apart they should be shortened enough to dissociate or the elementary fibril should untwist as a whole. In our experiments, the average length of the cellulose chains in the raw cotton was 6000–11000 residues and decreased to 1500–2000 residues after nitration. Thus, the lower bound estimate of the cellulose chain length was ~0.8–1.0 μm (O'Sullivan,

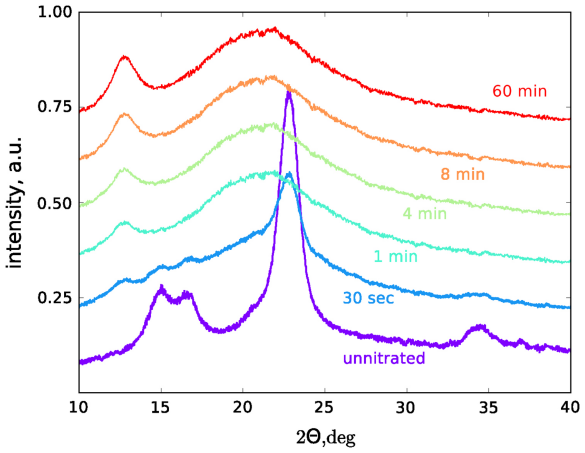

Fig. 3. X-Ray diffractograms of unnitrated cotton (purple) and cellulose nitrated for various time: 30 s (light-blue), 1 min (turquois), 4 min (green), 8 min (orange), and one hour (red). Curves were shifted for clarity.

1997) with the helix pitch being ~100 nm (Fernandes et al., 2011; Zhao et al., 2013). So, the cellulose macromolecules were held together by at least 8–10 turns. To assess quantitatively the effect of such twisting we can use a Capstan equation, that relates the frictional forces between the fibers F, friction coefficient k, and number of turns n:

$$F \sim e^{2\pi kn}$$

The friction coefficient between hydrogen-bonded cellulose chains is higher than the friction coefficient between two cellulose surfaces. Therefore, we can obtain a lower-bound estimate of the frictional forces between the cellulose chains in the nanofibril using a friction coefficient of ~0.5 (Stiernstedt et al., 2006). In this case, the frictional force restricting cellulose chains dissociation would be $\sim 10^{11}$ times greater than in case of the untwisted fiber. It means that a simple dissociation of cellulose macromolecules seems to be forbidden even in case of only 10 mutual twists. Thus, the nanofibril should be untwisted as a whole to allow the cellulose chains to dissociate. Since the characteristic time of the nitronium ion passing through the Born barrier is significantly higher than the nitration time, the access of the nitrating agents to the OH-groups in the bulk of the nanofibril is limited by the process of nanofibrils' swelling and untwisting.

The process of untwisting is related to the cellulose fibers swelling (Kasbekar & Neale, 1947; Mantanis, Young, & Rowell, 1994; Neale, 1933). The shape and characteristic time of wood swelling kinetic curves are very similar to the observed nitration kinetics (Mantanis et al., 1994) that confirms the relation between these two processes. This process is reversible and the native structure of cellulose is largely restored after removing the solvent (Neale, 1933). In the region of bulges formation the fiber does not only swell, but also untwists (Stovbun et al., 2016). Moreover, direct measurements demonstrate that the cotton fiber diameter grows in course of the nitration process (Fig. 4). The shape of the observed curve resembles the shape of the nitration kinetics (Fig. 2), but it can be approximated with only one exponential function and the characteristic time of this process is 8.1 ± 0.9 min. This value is by an order of magnitude close to the characteristic time of the second (slow) stage of the nitration process (Table 1). At the same time the fast component is absent here that clearly indicates the relation between the swelling and the second stage of nitration process.

The untwisted cellulose microfibrils in the nitrocellulose can be directly observed through an electron microscope (Fig. 5). This is a rather rare event, as the cellulose structure is generally stable under the nitration conditions (Fig. 1). Usually, the only common sign of swelling is the clearly visible cracks on the surface of the fibers ((Munro & Short, 1990), Fig. 1B, arrows). Nevertheless the cellulose structure on the edge

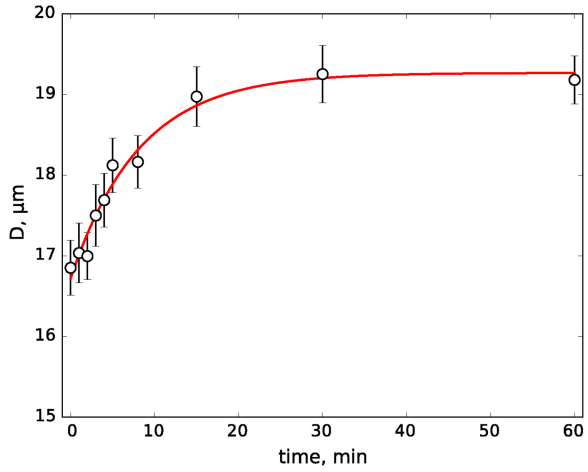

Fig. 4. Dependence of the cotton fiber diameter on the nitration time (295 K) according to optical microscopy observations. Bars are 95% credible intervals.

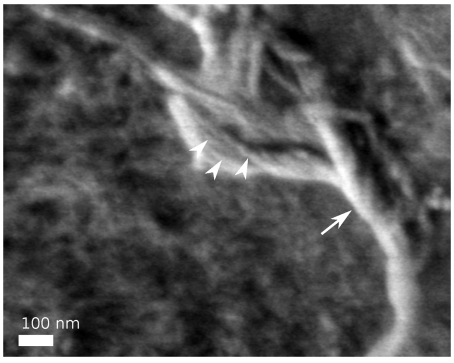

Fig. 5. Untwisted fiber in fully nitrated cotton cellulose pulp. The arrow marks the initial thick fiber of ~100 nm thick, while the arrowheads show the elementary fibrils of ~10 nm thick.

of the fibers is often disordered making the individual microfibrils visible (Fig. 5). We observed fibers of about 50 nm composed of several thinner fibers of about 10 nm (Fig. 5). The thin fibers can be interpreted as the nanofibrils and our estimate of their thickness (~10 nm) corresponds well to the previously reported on (~9 nm) obtained by the NMR (Newman, 1999). The helical structure of the microfibril as well as the twisting of the microfibrils to each other to form some thicker fiber (~100 nm) are clearly seen (Fig. 5). Unfortunately, we cannot directly demonstrate the dynamics of the untwisting process in the cellulose pulp during the nitration process, but it became possible to demonstrate the untwisted and ragged helical microfibril in the cellulose trinitrate. This observation is a strong argument in favor of the proposed mechanism of cellulose swelling through the untwisting of the nanofibrils.

Another confirmation is the increase of the amplitude of the nitration kinetics fast component in case of nitration of the dispersed wood cellulose (Sullivan et al., 2018; Trache et al., 2016). The nitrogen content in this case reached 12% in one minute, that is much faster than in case of untreated cotton cellulose. This effect could be explained by the cellulose nanofibrils loosening due to the process of dispersion that leads to the grow of the fraction of easily accessible hydroxyl groups.

4. Conclusion

The obtained quantitative estimates show that the diffusional restrictions cannot account for the cellulose nitration slow rate. Despite the low diffusion coefficient in the cellulose microcrystallites, their spatial dimensions are too small to explain the observed nitration rate decrease. However, the difference in the dielectric constants of the cellulose and nitrating mixture provides for a marked activation energy of the NO_2^+ transfer into the nanofibrils interior. This restriction would dramatically decrease the nitration rate and block nitration of nanofibrils interior in case their structure stays intact. The X-ray scattering experiments and the direct measurements of the cellulose fibers' thickness indicate the relation between the swelling and the nanofibrils interior nitration. The nanofibrils helical structure makes untwisting the only possible swelling way without cellulose chains breaking down. The untwisting of the whole nanofibril is a very slow process, as it harnesses the long macromolecules coordinated movements. The slow rate of untwisting correlates well with the long characteristic time of the cellulose nitration at the second stage.

The proposed mechanism allows to propose a way of improving the raw cellulose. Any factor intensifying the dissociation of macromolecules would increase the cellulose quality including the appearance of additional uncompensated charges on the fibrils surfaces after the sulfite treatment, as it was shown earlier (Stovbun et al., 2016).

References

Balser, K., Hoppe, L., Eicher, T., Wandel, M., Astheimer, H., Steinmeier, H., & Allen, J. (2012). *Cellulose esters. Ullman's encyclopedia of industrial chemistry*. Weinheim, Germany: Wiley-VCH Verlag GmbH & Co. KGaA.

Barbosa, I., Merquior, D., & Peixoto, F. (2005). Continuous modeling and kinetic parameter estimation for cellulose nitration. *Chemical Engineering Science, 60*, 5406–5413.

Belova, E., Vais, N., Sopin, V., Kazakov, A., Rubtsov, Y., Manelis, G., & Marchenko, G. (1989). Kinetics and mechanism of nitration of cellulose with the hno_3-ch_2cl_2 mixture. *Bulletin of the Academy of Sciences of the USSR, 38*, 2244–2249.

Edwards, H., & Fawcett, V. (1994). Quantitative Raman spectroscopic studies of nitronium ion concentrations in mixtures of sulphuric and nitric acids. *Journal of Molecular Structure, 326*, 131–143.

Fernandes, A., Thomas, L., Altaner, C., Callow, P., Forsyth, V., Apperley, D., Kennedy, C., & Jarvish, M. (2011). Nanostructure of cellulose microfibrils in spruce wood. *Proceedings of the National Academy, 108*, E1195–E1203.

Gert, E., Matyulko, A., Shishonok, M., Zubets, O., & Kaputskii, F. (2003). Nitric acid procedure for production of powdered cellulose ii forms with various morphologies and comparison of their structural and sorption characteristics. *Russian Journal of Applied Chemistry, 76*, 1337–1343.

Gillespie, R., & Cole, R. (1956). The dielectric capacity constant of sulphuric acid. *Transactions of the Faraday Society, 52*, 1325–1331.

Hanley, S. J., Giasson, J., Revol, J.-F., & Gray, D. G. (1992). Atomic force microscopy of cellulose microfibrils: Comparison with transmission electron microscopy. *Polymer, 33*, 4639–4642.

Hanley, S. J., Revol, J.-F., Godbout, L., & Gray, D. G. (1997). Atomic force microscopy and transmission electron microscopy of cellulose from *Micrasterias denticulata*: Evidence for a chiral helical microfibril twist. *Cellulose, 4*, 209–220.

Hughes, E., Ingold, C., & Pearson, R. (1958). Nitration at nitrogen and oxygen centres. Part I. Kinetics and mechanism of the conversion of secondary amines into nitroamines. *Journal of the Chemical Society*, 4357–4365.

Ingold, C. K. (1953). *Mechanisms of nitration. Structure and mechanism in organic chemistry*. New York: Cornell University Press269–288 (chapter 21).

Ishida, Y., Yoshino, M., Takayanagi, M., & Irie, F. (1959). Dielectric studies on cellulose fibers. *Journal of Applied Polymer Science, 1*, 227–235.

Kasbekar, G., & Neale, S. (1947). The swelling of cellulose in aqueous solutions of certain acids and salts with measurements of the vapour pressures, densities and viscosities of these solutions. *Transactions of the Faraday Society, 43*, 517–528.

Kovalenko, V. (1995). Inhomogeneity in the molecular structure of cellulose nitrates. *Russian Chemical Reviews, 64*, 753–766.

Mantanis, G., Young, R., & Rowell, R. (1994). Swelling of wood. Part 1. Swelling in water. *Wood Science and Technology, 28*, 119–134.

Meader, D., Atkins, E., & Happey, F. (1978). Cellulose trinitrate: Molecular conformation and packing considerations. *Polymer, 19*, 1371–1374.

Mikhailov, A., Bel'kova, L., & Gromov, S. (1980a). Polychronous kinetics of wood delignification. 1. Nitric-acid delignification. *Khim Drev, 6*, 50–58 (in Russian).

Mikhailov, A., Bel'kova, L., & Gromov, S. (1980b). Polychronous kinetics of wood delignification. 2. Diffusional kinetics of nitric-acid delignification. *Khim Drev, 6*, 59–64 (in Russian).

Muhlethaler, K. (1967). Ultrastructure and formation of plant cell walls. *Annual Review of Plant Biology, 18*, 1–24.

Munro, H., & Short, R. (1990). A study of the low temperature nitration of cellulose in mixed acids. *Journal of Applied Polymer Science, 39*, 539–551.

Murch, G. (1984). *Diffusion in crystalline solids*. New York: Academic Press.

Neale, S. (1933). The modification of natural cotton cellulose by swelling and by degradation. *Transactions of the Faraday Society, 29*, 228–234.

Newman, R. (1999). Estimation of the lateral dimensions of cellulose crystallites using ^{13}C NMR signal strengths. *Solid State Nuclear Magnetic Resonance, 15*, 21–29.

O'Sullivan, A. C. (1997). Cellulose: The structure slowly unravels. *Cellulose, 4*, 173–207.

Preston, R. (1934). The organisation of the cell wall of the conifer tracheid. *Philosophical*

Transactions of the Royal Society B, 61, 131–174.
Rafeev, V., Rubtsov, Y., Sorokina, T., & Chukanov, N. (1999). Equilibrium constants of cellulose nitration by nitric acid under quasi-homogeneous conditions. *Russian Chemical Bulletin, 48*, 66–70.
Richter, G. (1929). Process for the production of high-alpha cellulose fiber for the manufacture of cellulose derivatives. US1741540 A.
Ruben, G., & Bokelman, G. (1987). Triple-stranded, left-hand-twisted cellulose microfibril. *Carbohydrate Research, 160*, 434–443.
Saren, M., Serimaa, R., Andersson, S., Paakkari, T., & Pesonen, P. S. E. (2001). Structural variation of tracheids in Norway spruce (*Picea abies* [l.] Karst.). *Journal of Structural Biology, 136*, 101–109.
Sasi, J., & Chanzy, H. (1995). Ultrastructural aspects of the acetylation of cellulose. *Cellulose, 2*, 111–127.
Saunders, C., & Taylor, L. (1990). A review of the synthesis, chemistry and analysis of nitrocellulose. *Journal of Energetic Materials, 8*, 149–203.
Short, R., & Munro, H. (1990). Aspects of the surface and bulk nitration of cellulose in nitric acid, nitric acid/water, and nitric acid/dichloromethane mixes. *Journal of Applied Polymer Science, 39*, 1973–1982.
Short, R., & Munrot, H. (1993). Conclusions drawn from a study of cellulose nitration in technical mixed acids by X-ray photoelectron spectroscopy and ^{13}C nuclear magnetic resonance. *Polymer, 34*, 2714–2719.
Somerville, C. (2006). Cellulose synthesis in higher plants. *Annual Review of Cell and Developmental Biology, 22*, 53–78.
Stiernstedt, J., Nordgren, N., Wagberg, L., Brumer, H., Gray, D., & Rutland, M. (2006). Friction and forces between cellulose model surfaces: A comparison. *Journal of Colloid and Interface Science, 303*, 117–123.
Stovbun, S. V., Nikolsky, S. N., Melnikov, V. P., Mikhaleva, M. G., Litvin, Y., Shchegolikhin, A., Zlenko, D. V., Tverdislov, V., Gerasimov, D., & Rogozin, A. (2016). Chemical physics of cellulose nitration. *Russian Journal of Physical Chemistry B, 10*, 245–259.
Sullivan, F., Simon, L., Ioannidis, N., Patel, S., Ophir, Z., Gogos, C., Jaffe, M., Tirmizi, S., Bonnett, P., & Abbate, P. (2018). The nitration kinetics of cellulose fibers derived from wood pulp in mixed acids. *Industrial and Engineering Chemistry Research, 57*, 1883–1893.
Thomas, L., Forsyth, V., Sturcova, A., Kennedy, C., May, R., Altaner, C., Apperley, D., Wess, T., & Jarvis, M. (2013). Structure of cellulose microfibrils in primary cell walls from collenchyma. *Plant Physiology, 161*, 465–476.
Trache, D., Khimeche, K., Mezroua, A., & Benziane, M. (2016). Physicochemical properties of microcrystalline nitrocellulose from Alfa grass fibres and its thermal stability. *Journal of Thermal Analysis and Calorimetry, 124*, 1485–1496.
Urbansky, T. (1965). *Nitration of cellulose. Chemistry and technology of explosives*, *Vol. 2*, Oxford: Pergamon Press321–361 (chapter XII).
Whorlow, R. (1980). *Rheological techniques.* Chichester, UK: Ellis Horwood.
Zhao, Z., Shklyaev, O., Nili, A., Mohamed, M., Kubicki, J., Crespi, V., & Zhong, L. (2013). Cellulose microfibril twist, mechanics, and implication for cellulose biosynthesis. *Journal of Physical Chemistry A, 117*, 2580–2589.